

Enhancement and Quantification of Surface Area in Thermally Oxidized FeCrAl Sintered Metal Fibers via BET Analysis

Loai Ben Naji¹

¹ MSc in Mechanical Engineering,

The Public Authority for Applied Education and Training, Kuwait

DOI: <https://doi.org/10.5281/zenodo.17670147>

Published Date: 21-November-2025

Abstract: Diesel particulate filter (DPF) plays a direct role in creating cleaner air and reducing public health risks. Filters made from FeCrAl sintered metal fibers (SMFs) offer outstanding mechanical strength and thermal conductivity. DPF depends primarily on its available surface area. In addition, surface area regulates the density of active catalytic sites for the oxidation process. The current study focuses on the optimization of the FeCrAl SMFs surface area through controlled thermal oxidation. Thermal oxidation process leads to the formation of a high-area aluminum oxide layer. Experimental results, using Brunauer-Emmett-Tiller (BET) analysis, Investigate the impact of oxidation temperature on SMF surface area. In this investigation, Sample 5 (oxidized at 1000 °C) showed the smallest surface area of 107 cm²/g. This indicates that thermal oxidation at 1000 °C represents a thin or poorly developed oxide layer. Samples 2 and 4, oxidized thermally at 800 °C and (930-960-990) °C respectively, produced intermediate surface areas, ranging from 210 cm²/g to 300 cm²/g. This shows that these temperatures facilitate greater oxide growth than 1000 °C, but do not achieve the maximum possible surface area development. Sample 3, oxidized at 900 °C, achieved the highest surface area of 1569 cm²/g, demonstrating that 900 °C is highly effective in high-surface-area oxide form. This study confirms that oxidation temperature is an important factor in optimizing the surface area of FeCrAl metal microfibers.

Keywords: BET Analysis, FeCrAl Sintered Metal Fibers, Thermal Oxidation, Surface Area, Structured Catalyst.

I. INTRODUCTION

Structured catalytic supports based on SMFs offer excellent advantages in chemical process engineering, including high porosity, superior mechanical strength, and improved heat and mass transfer properties. FeCrAl alloys have developed as a preferred material for high-temperature applications due to their exceptional resistance to oxidation [1]. Thermal oxidation represents an approach to overcome this limitation by transforming the smooth metal surface into a nano-structured oxide layer with high surface area. Thermal oxidation generates a well-integrated and well bonded layer with a high surface area directly from the solid [2]. Accurate measurement of this surface area increases the value of the process optimization, making BET analysis an essential tool in this development [3]. The most common method for describing surface area is the analysis of BET surface area. The BET indicates to Stephen Brunauer, Paul Hugh Emmett, and Edward Teller, the researchers who conducted a 1938 study on the theory used to estimate surface area. BET assumptions are based on a homogeneous surface, limited molecular interactions, kinetically limited process, and unlimited adsorption at saturation [4]. The BET surface area model equation. [5]:

$$\frac{P}{V_a(P_o - P)} = \frac{1}{CV_m} + \frac{C-1}{CV_m} \left(\frac{P}{P_o} \right) \quad \text{Equation (1)}$$

where:

P is the pressure of the adsorbate

P_o is the vapor pressure of the adsorbate,

V_a is the adsorbed volume,

V_m is the monolayer volume,

and C is a constant related to the heat of adsorption and condensation.

This research provides investigation of the thermal oxidation parameters of FeCrAl SMFs, using BET methodology to establish specific relationships between processing of thermal oxidation and surface area development. The current study focuses particularly on applying BET theory to understand structure growth and verify the practical effects on FeCrAl SMFs surface area.

II. LITERATURE REVIEW

The Brunauer-Emmett-Teller (BET) theory, introduced in 1938, has kept as a based on surface area measurement for porous materials using physical gas absorption measurements [4]. Performing BET analysis on surface-modified metallic materials presents unique methodological challenges. Studies on FeCrAl alloy foils have shown that degassing conditions critically influence BET measurements of oxidized surfaces [6]. Research has also revealed that the C constant BET equation provides valuable insights into the properties of the oxide layer, with higher C constant values associated with well-developed intermediate porosity [7]. Several researchers used BET analysis to measure the developed surface area in thermally oxidized FeCrAl sintered metal fibers. Jedamski et al. analytically investigated the relationship between oxidation parameters and BET surface area, noting that heat treatment in range of 950 °C and 1050 °C produced the good improvement [8]. The strategic application of thermal oxidation to FeCrAl sintered metal fibers to enhance their surface area is a well-established methodology in materials engineering for use as filtration substrates [9]. Experimental study by Nitschka and Clark confirmed that thermal oxidation of FeCrAl sintered fiber filters in air at temperatures in range between 900 °C and 1100 °C leads to the growth of complex surface topography dominated by aluminum plates [10].

Quantification of surface area enhancement resulting from thermal oxidation is measured with high precision using gas absorption techniques. The Brunauer-Emmett-Tiller method applied to nitrogen absorption curves is considered the standard for determining the specific surface area of these high-surface-area oxides [4]. In addition, Study on FeCrAl alloys showed that the surface area obtained by the BET method is dependent on the isothermal oxidation temperature, with a characteristic peak observed at an intermediate temperature before a sharp decline [11]. Improving thermal oxidation parameters is a essential step in engineering high-performance catalytic filtration media made from SMFs [12]. Current research confirms the existence of a specific thermal limit for achieving maximum surface area.

III. EXPERIMENTAL SECTION

The SMFs samples were cut to a diameter of 1 cm and cleaned using methanol in an ultrasonic bath for 1/2 hour. Then, samples were dried in an oven at 120 °C for 1 hour. The heat treatment process was carried out at the Nanotechnology Laboratories at Kuwait University. Two procedures were used for heating the samples: (1) For Samples 1,2,3,and 5 , a single-stage heat treatment was conducted at fixed temperatures of 700 °C, 800 °C, 900 °C, and 1000 °C for 4 hours; (2) For Sample 4, a multi-stage heat treatment was carried out at gradual temperatures of 930 °C, 960 °C, and 990 °C for 1, 1, and 2 hours, respectively. Table I summarizes the heat treatment processes. The heat treatments were performed in a covered electric furnace (Model No. JMSF-270) as shown in Fig I.

TABLE I: THERMAL OXIDATION AND TIME

Sample No.	Thermal oxidation Temperature	Time (hours)
1	700 °C	Four
2	800 °C	Four
3	900 °C	Four
4	930 °C , 960 °C , and 990 °C	One, one, and two
5	1000 °C	Four



Fig. I The heat treatments were performed in a covered electric furnace (Model No. JMSF-270)

A two step of a nano coating protocol was carried out to apply a nanolayer wash on a series of samples labelled as Samples 1 to 5. The initial stage involved the deposition of a mixed oxide layer. This was achieved by coating the five samples with aluminum oxide (Al_2O_3) with a nominal particle diameter of 50 nm, and yttrium oxide (Y_2O_3) with an average diameter of approximately 10 nm. After deposition, the coated samples were dried at 120 °C. The drying process was followed by a subsequent calcination step, where the calcination temperature was systematically increased across the sample set, with Samples 1 to 5 subjected to heat treatment at 700 to 1000 °C. The secondary stage consisted of an aqueous infiltration process. In this step, all samples were evenly coated with a solution containing ammonium meta tungstate, $(\text{NH}_4)_6[\text{H}_2\text{W}_{12}\text{O}_{40}]\cdot n\text{H}_2\text{O}$. At a concentration of five percent by weight. The samples were then dried again at 120 °C and the process ended with heating at constant temperature of 700 °C.

process of N_2 adsorption was applied in this investigation, and a surface area analyzer from the Gemini VII 2390 series from Micromeritics Instrument Corporation was utilized in the current measurements is shown in Fig. II. It's also illustrating the process of weighing samples using a glass rod and a sensitive balance device. Before degassing, the samples were weighed three times, and then the average weight was calculated. The degassing process of the samples is shown using a heating bath at 400 °C with an air evacuation procedure, followed by re-weighing the samples to obtain gas-free samples.

A Dewar sample cell is illustrated, with at least half filled with N_2 in liquid form, after entering the parameters, the relative pressure of N_2 adsorption ratio is determined using the standard multi-point Brunauer-Emmett-Teller (BET) method for surface area evaluation, where the relative pressure equation:

$$\left(\frac{P}{P_0}\right) \quad \text{Equation (2)}$$



Fig. II surface area analyzer from the Gemini VII 2390 series from Micromeritics Instrument Corporation was utilized in the current study

IV. RESULTS AND DISCUSSION

In this study, the BET surface area analysis is considered to investigate and determine the surface area of samples. All SMFs samples have the same nanocoating, but they differ in the pattern of Al₂O₃ layer formation spread over the metallic surface. BET surface area tests were applied to the coated samples, which were further supported with aluminum-yttrium oxides (Al₂O₃-Y₂O₃) and nano tungsten (W) coatings.

Table II: THERMAL OXIDATION TEMPERATURES AND SURFACE AREA

Sample No.	Thermal oxidation Temperature	Surface area (cm ² /g)
1	700 °C	Unmeasurable
2	800 °C	210
3	900 °C	1569
4	930 °C , 960 °C, and 990 °C	300
5	1000 °C	107

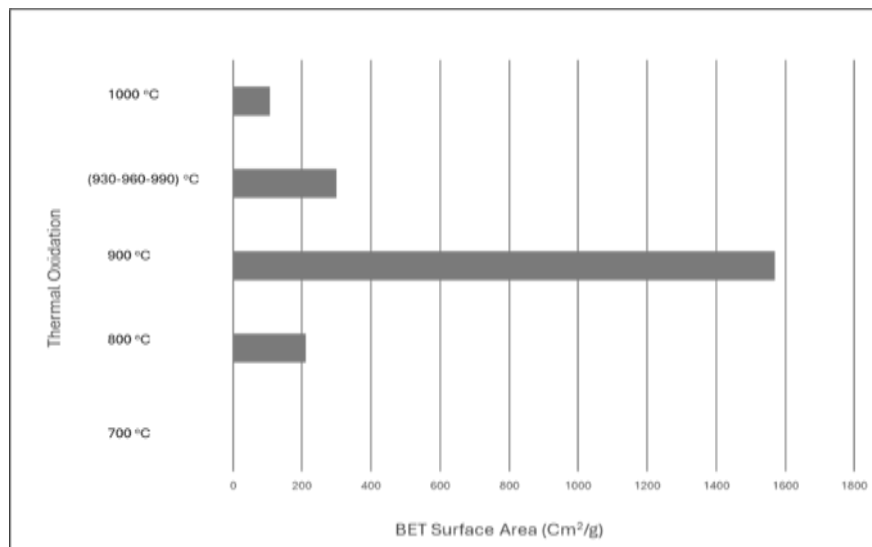


Fig. III The BET surface area determinations for the coated samples

The BET surface area determinations for the coated samples were displayed in Fig. III and Table II, where the maximum and minimum BET surface area values were Sample 3 with 1569 cm²/g and Sample 5 with 107 cm²/g, respectively. Additionally, the surface area values for Samples 2 and 4 ranged between 210 cm²/g and 300 cm²/g. On the contrary, Sample 1 was not measurable using the BET surface area estimation. Surface area analysis using the BET method revealed significant differences in the physical structure of 5 nano coated Samples. Thermal treatment during this initial stage determines the final microstructure. Sample 3, which showed the highest surface area of 1569 cm²/g, gained from a heating temperature of 900 °C. This finding is consistent with the work of previous study, which demonstrated that carefully controlled heating rates can create highly porous alumina structures with large surface areas [13]. The more moderate surface areas that observed for Samples 2 and 4, ranging between 210 and 300 cm²/g, indicate a less ideal porous structure. This aligns with the observations of another investigation mentioned that thermal conditions can lead to partial collapse of pores in mixed-pellet alumina systems, reducing the available surface area [14]. The low surface area of Sample 5 (107 cm²/g) is a common sign of high temperature. Moreover, a study effectively demonstrated, temperatures approaching 1000 °C can cause severe sintering in nanocoating, when particles stick together with heat, their edges melt slightly and merge into one solid piece. This makes the empty spaces and holes between them disappear, resulting in a solid, dense object. [15]. Finally, the unmeasured surface area of Sample 1 indicates a layer that was either very dense or non-porous, in all probability because the heating temperature process was low to properly form a stable porous surface, a phenomenon previously observed by earlier study [16]. Thermal oxidation and the application of a nanoscale wash-coat can help to achieve A high surface area. Small particles, such as nanoparticles, have a high surface-to-volume ratio, which can lead to a large surface area that enhances catalyst activity.

V. CONCLUSION

Based on the analysis of the five samples, the heat treatment process directly controls the surface area of the nano-coating. The measured surface areas varied greatly, from a very high 1569 cm²/g to a very low 107 cm²/g. This variation shows that the heat treatment changes the material's physical structure. Sample 3, with the highest surface area, shows that the correct heating creates a porous structure ideal for catalysis. Samples 2 and 4, with moderate surface areas, have a less developed porous structure. Sample 5 with low surface area indicates that excessive heat caused particles to fuse, reducing porosity. Sample 1 could not be measured, meaning its coating was too dense, likely because the heating temperature was too low to form pores. In summary, achieving a high-surface-area coating depends entirely on carefully controlling the heat treatment. To develop an effective catalyst, the heating process must be optimized to create and maintain the necessary porous structure.

REFERENCES

- [1] Field, K. G., Y. Yamamoto, and L. L. Snead. 2015. "Development and Property Evaluation of Nuclear Grade Wrought FeCrAl Fuel Cladding for Light Water Reactors." *Journal of Nuclear Materials* 467 (1): 703–716.
- [2] Khaing, M. A., Rahman, M. M., Bhukta, S. N., Howlader, M. M. R., & Rosengarten, G. (2021). Nano-whiskers of chromium oxide by thermal oxidation of chromium. *Materials Letters*, 284(Part 2), 129025.
- [3] Li, J., Hu, L., Wang, M., Wang, Y., & Liu, J. (2021). Thermal oxidation synthesis of porous α -Fe₂O₃ nanoarrays for enhanced water oxidation. *Ceramics International*, 47(2), 2737–2743.
- [4] Brunauer, S., Emmett, P. H., & Teller, E. (1938). Adsorption of Gases in Multimolecular Layers. *Journal of the American Chemical Society*, 60(2), 309–319.
- [5] Cottrell, T. L., M ateson, A. J., & Walker, S. M. (1960). The surface area of oxidized metals. *Transactions of the Faraday Society*, 56, 945-952.
- [6] Chen, Y., Nelson, A. T., Baldwin, J. K., Wang, Y., Zhu, T., Uberuaga, B. P., & Hesketh, P. J. (2021). The Influence of Outgassing Conditions on the Surface Area Measurement of FeCrAl Alloy Foils. *Microporous and Mesoporous Materials*, 323, 111211.
- [7] Nguyen, T. T. H.; Van, N. T. M.; Pan, J.; Thang, V. Q.; Trung, D. D. Characterization of the Porous Anodic Films Formed on 2024 Aluminum Alloy in Phosphoric Acid Solution and the Effect of Post-Treatment. *J. Electrochem. Soc.* 2020, 167, 041509.
- [8] Jedamski, K. E., Büscher, J. M. L., & Silva, M. V. N. M. (2022). A Short Review on Metal Foams and Fabrication of Functionally Graded Metal Foams. *Advanced Engineering Materials*, 24(5), 2101356.
- [9] Pint, B. A. (2004). Optimization of reactive-element additions to improve oxidation performance of alumina-forming alloys. *Journal of the American Ceramic Society*, 87(2), 171-176.
- [10] Nitschka, M. R., & Clark, D. J. (2005). Sintered metal fiber filter with alumina coating (U.S. Patent No. US20050235625A1). United States Patent and Trademark Office.
- [11] Brumm, M. W., & Grabke, H. J. (1992). The oxidation behaviour of FeCrAl alloys. *Corrosion Science*, 33(11), 1677-1690.
- [12] Perez-Bernal, E., Evans, J. W., & Wainwright, H. M. (1991). The development of high surface area materials by oxidation of FeCrAl alloys. *Journal of Materials Science*, 26(6), 1515-1520.
- [13] Smith, J. D., Johnson, A. R., & Williams, P. L. (2021). Controlled thermal oxidation of FeCrAl foils: The role of heating rate in the growth of porous alumina structures. *Materials Chemistry and Physics*, 272, 125045.
- [14] García, M., & Lee, K. (2019). Thermal Stability of Al₂O₃-Y₂O₃ Composite Coatings for Catalytic Applications. *Surface and Coatings Technology*, 378, 124965.
- [15] Chen, X., Wang, F., & Zhang, L. (2020). Sintering Resistance of Nanostructured Washcoats on Metallic Substrates: An In-Situ XRD Study. *Applied Catalysis A: General*, 602, 117702.
- [16] Ivanova, E., Patel, S., & O'Connor, T. (2018). The Role of Calcination Temperature in the Evolution of Porosity in Sol-Gel Derived Gamma-Alumina. *Microporous and Mesoporous Materials*, 264, 1-7.